Role of Sindbis Virus Capsid Protein Region II in Nucleocapsid Core Assembly and Encapsidation of Genomic RNA[▽]

Ranjit Warrier,[1] Benjamin R. Linger,[2]† Barbara L. Golden,[2] and Richard J. Kuhn[1]*

Markey Center for Structural Biology, Department of Biological Sciences, 915 W. State Street,[1] and Department of Biochemistry, 175 S. University Street,[2] Purdue University, West Lafayette, Indiana 47907

Sindbis virus is an enveloped positive-sense RNA virus in the alphavirus genus. The nucleocapsid core contains the genomic RNA surrounded by 240 copies of a single capsid protein. The capsid protein is multifunctional, and its roles include acting as a protease, controlling the specificity of RNA that is encapsidated into nucleocapsid cores, and interacting with viral glycoproteins to promote the budding of mature virus and the release of the genomic RNA into the newly infected cell. The region comprising amino acids 81 to 113 was previously implicated in two processes, the encapsidation of the viral genomic RNA and the stable accumulation of nucleocapsid cores in the cytoplasm of infected cells. In the present study, specific amino acids within this region responsible for the encapsidation of the genomic RNA have been identified. The region that is responsible for nucleocapsid core accumulation has considerable overlap with the region that controls encapsidation specificity.

Members of the alphavirus genus are distributed throughout the world and cause encephalitis, rashes, and arthritis in humans (31). Chikungunya virus, a member of this genus, recently caused an epidemic on the Indian Ocean island of Reunion (28). The alphaviruses are composed of a T=4 icosahedral nucleocapsid core (NC) that contains the genomic RNA of the virus. Surrounding the NC is a host-derived lipid bilayer. The glycoproteins E1 and E2, responsible for membrane fusion and receptor recognition, respectively, span this lipid membrane (3, 16, 19, 23, 41).

The capsid protein (CP) of alphaviruses is a multifunctional protein, acting at different stages in the viral life cycle. It has been shown to act as an autoprotease, to recognize the genomic RNA, and to assemble into an ordered protein shell forming the NC. The NC interacts with viral glycoproteins to produce mature virus. Upon entry into a new host, alphaviruses undergo fusion in the low-pH environment of the endosome and release NCs into the cytoplasm, where they disassemble and release the RNA genome. Although there appear to be different functional domains, some of these activities may correspond to overlapping regions of amino acid residues. In the Sindbis virus (SINV) CP, the protease domain and the region that interacts with glycoproteins have been identified but the regions that specify genome RNA recognition and NC assembly have yet to be fully characterized (34).

CP is the first structural protein to be translated from subgenomic RNA, and it cotranslationally cleaves itself from the nascent structural polyprotein (1, 20). The CP then binds to genomic RNA, promoting NC formation. Interaction between the NC and glycoproteins occurs on cellular membranes and results in the budding and release of the virus (31). NCs accumulate in the cell, presumably because the rate of NC assembly is greater than the rate of virus budding. An alternative model of virus assembly, in which the glycoproteins organize CP and genomic RNA into NCs at the plasma membrane and the observed NCs in the cytoplasm are dead-end products, has also been proposed previously (7, 8).

One of the difficulties in dissecting the pathway of the assembly of SINV NC from CP and RNA is the inability to isolate assembly intermediates in vivo. The nucleic acid binding event is proposed to be the first step in initiating the assembly process, as NCs devoid of RNA have not been found either by analyzing infected cells or by using in vitro assembly assays (32, 33, 38). The CP recognition of genomic RNA leads to CP-CP interactions and the encapsidation of this RNA. From the results of in vitro RNA binding assays, it is known that the amino acid region from positions 81 to 112 recognizes an encapsidation signal on the genomic RNA (14, 36, 37). A deletion of residues 97 to 106 in SINV CP results in a virus that has lost its ability to recognize the genomic RNA, and the replacement of leucine residues at positions 108 and 110 with glutamate and asparagine results in a failure to accumulate NCs in the cytoplasm (13, 22). In Semliki Forest virus, a related alphavirus, deletions of residues 100 to 105, 106 to 113, and 100 to 113 (SINV numbering) cause defects in NC accumulation (2). The mutation of residues corresponding to SINV CP positions 108 and 110 to alanines in Semliki Forest virus CP also results in the inhibition of NC accumulation (30). Since no NCs devoid of nucleic acid have been found and CP is monomeric in the absence of nucleic acid, CP-nucleic acid interactions are considered to be the initial events in NC assembly. As the region comprising positions 81 to 113 has been implicated in the specific recognition of genomic RNA, this region is considered to be an initiator region in NC assembly.

A model of SINV NC assembly based on in vitro results suggests that the NC is formed from a nucleation event in which a monomer of CP binds to an encapsidation signal on

* Corresponding author. Mailing address: Markey Center for Structural Biology, Department of Biological Sciences, Purdue University, 915 W. State St., West Lafayette, IN 47907. Phone: (765) 494-1164. Fax: (765) 496-1189. E-mail: kuhnr@purdue.edu.

† Present address: Department of Molecular Genetics, Biochemistry and Microbiology, University of Cincinnati, Cincinnati, OH.

the genomic RNA. This interaction exposes a second site on the encapsidation signal for binding by another molecule of CP (14). Subsequently, CP dimerization events in the region comprising residues 81 to 113 and in the helix I region (residues 38 to 55) of CP take place. The remaining steps of this process are unknown (10, 14, 25, 35). This model predicts that the amino acids responsible for the nucleic acid recognition and the CP dimerization are within the region from positions 81 to 113. A genetic approach was selected to determine if the region corresponding to nucleic acid recognition and the region corresponding to CP dimerization overlap or are distinct. Initially, we engineered deletion mutations throughout these regions to remove amino acids that may be responsible for either nucleic acid recognition or CP dimerization. For a better understanding of the specific roles of amino acids in these processes, we replaced conserved residues, individually or in combination, and analyzed the defects of the generated viruses.

MATERIALS AND METHODS

Viruses and cells. Viruses were grown in baby hamster kidney cell line 15 (BHK) cells in Eagle's minimal essential medium supplemented with 10% fetal bovine serum unless otherwise indicated.

Construction of mutant viruses. Mutations were constructed in pToto64, the full-length cDNA clone of SINV, by overlap PCR (13, 22). The size of the PCR products was approximately 1,000 bp. The mutations were confirmed by sequencing a region of 1,000 nucleotides that included the entire coding sequence for CP. RNA was produced by in vitro transcription, and BHK cells were transfected with the RNA by using DEAE-dextran (12). The resulting viruses were plaque purified twice, and viral stocks were generated from the second round of plaque-purified samples. The presence of the mutation in each virus was confirmed by sequencing the reverse transcriptase PCR (RT-PCR) products corresponding to the CP coding region from RNA purified from cytoplasmic extracts of infected BHK cells. These viral stocks were then used for further experiments. The naming of the viruses was as suggested by Kuhn et al. (11). For example, a mutant virus carrying a 5-amino-acid deletion of residues 101 to 105 in CP is referred to as $C\Delta(101–105)$.

One-step growth analyses. Virus replication was examined by one-step growth analyses as described previously, with the exception that cells were infected at a multiplicity of infection of 2 (11). Following the adsorption of the viruses to the cells for 1 h at room temperature, the cells were placed at 37°C, and the medium was replaced every 30 min for the first 2 h and every hour thereafter until the 12-h time point. Titers of released virus were determined by plaque assays of BHK cell monolayers. The assays were carried out in duplicate. The results reported are the averages of the two titers obtained for each time point.

NC accumulation assay. BHK cells were electroporated with full-length wild-type and mutant viral RNA to avoid bias due to defects in entry or in uncoating associated with virus infection. The cells that were transfected with each RNA were divided into two groups immediately, and the RNA produced in one group was labeled with [5,6-^{3}H]uridine. The second group was used to determine the electroporation efficiency by an immunofluorescence assay using a polyclonal antibody that recognizes the cytoplasmic domain of glycoprotein E2 (kindly provided by Milton Schlesinger). Cytoplasmic extracts were prepared at 12 h postelectroporation. Labeled NCs were purified by the centrifugation of cytoplasmic extracts through a 10 to 40% sucrose density gradient. The gradients were fractionated manually, and then each fraction was subjected to scintillation counting (15).

qRT-PCR. A quantitative real-time RT-PCR (qRT-PCR) assay was performed using the SuperScript III Platinum one-step qRT-PCR system (Invitrogen Corporation, Carlsbad, CA) according to a protocol modified from one by Pastorino et al. (24). All experiments were conducted on an Applied Biosystems 7300 real-time PCR system (Applied Biosystems, Foster City, CA). Primers were selected using Primer Express software (Applied Biosystems, Foster City, CA), synthesized by Integrated DNA Technologies (Coralville, IA), and tested for detection levels by using dilutions of virus-containing cell culture supernatants. The primers with the lowest standard deviations in three experiments were used in subsequent experiments. Specific to the genomic RNA sequence were forward primer 5′-TTCCCTGTGTGTGCACGTACAT-3′ and reverse primer 5′-TGAGCC CAACCAGAAGTTTT-3′. Primers that bound to regions in both the genomic

RNA and the subgenomic RNA were forward primer 5′-GCGTCATTGACGA CTTTACCC-3′ and reverse primer 5′-CCCAGACCTGCTCGATCTTAA-3′. Standard curves of the cycle threshold (C_T) versus the number of molecules of RNA were determined by assaying known amounts of in vitro-transcribed and purified genomic RNA. Amounts of genomic and subgenomic RNAs in the mutant viruses were determined from these standard curves, and the ratios of subgenomic RNA to genomic RNA were calculated. Each experiment was conducted at least nine times, using samples generated at different time points and at different dilutions.

In vitro transcription of encapsidation signal RNA. A plasmid containing the encapsidation signal sequence of SINV was kindly provided by Sondra Schlesinger (36). Two DNA oligomers were synthesized to amplify the region from nucleotides 945 to 1076 by PCR. The amplified and digested product was ligated into pUC19 (New England Biolabs) between the unique HindIII and XbaI restriction sites. In addition to the desired complementary nucleotides, the 5′ oligomer contained a HindIII restriction site upstream of a T7 promoter and also included the addition of three nucleotides, GGA, at the start site for the enhancement of transcription. The 3′ oligomer contained an EarI digestion site for the generation of the desired 3′ end for runoff transcription. *Escherichia coli* strain XL1-Blue was then transformed with the ligation products. Insert-containing clones were sequenced to verify that the amplified region was inserted correctly. Plasmid purification was performed using the Qiagen Giga-Prep kit. The plasmid was linearized by EarI digestion and extracted with phenol-chloroform prior to the use of the plasmid in transcription reactions. RNA was synthesized using T7 RNA polymerase as previously described (17). RNAs for use in mobility shift assays were radiolabeled with ^{32}P either by the labeling of the 5′ end with [γ-^{32}P]ATP and polynucleotide kinase (Promega) or by the incorporation of [α-^{32}P]ATP during in vitro transcription.

Cloning, expression, and purification of CP(81–112) mutant peptides. The peptide comprising amino acid residues 81 to 112 of the SINV CP [CP(81–112)] was expressed as an Smt3 fusion protein from a modified pET28b vector (18). Two DNA oligomers were synthesized to amplify the nucleotide sequence encoding amino acid residues 81 to 112 of the SINV CP. Site-directed mutagenesis was achieved by modifying the required nucleotides of either one or both of the DNA oligomers. Amplified and digested products were ligated into the modified pET28b vector between unique BamHI and HindIII restriction sites. *E. coli* strain XL1-Blue was transformed with the ligation products. Clones were sequenced to verify that the fragments were inserted correctly, and *E. coli* strain BL21(DE3) was transformed with the correctly constructed plasmids for protein expression. The fusion protein was isolated using a Ni-agarose affinity column and cleaved at 4°C for 6 h with Ulp1 protease by using a 1,000:1 ratio, by mass, of fusion protein to protease. Ulp1 was expressed and purified as previously described (18). The cleaved capsid fragment was loaded onto a HiTrap SP HP column (Amersham) and equilibrated with 25 mM Tris-HCl (pH 8.0)–100 mM NaCl. The protein was eluted with a linear salt gradient from 100 mM to 1 M NaCl in 25 mM Tris-HCl (pH 8.0). Fractions containing CP fragments were concentrated with Centricon YM-3 centrifugal filter devices at 4°C and exchanged into 25 mM HEPES (pH 7.4)–150 mM potassium acetate. Protein concentrations were determined by measuring absorption at 215 nm (ε_{215} = 41,000 $M^{-1}cm^{-1}$).

Mobility shift assay for measuring encapsidation signal RNA binding affinities of mutant peptides. For band-shift assays with the CP(81–112) mutant peptides, samples were 10 μl in volume and contained 0.2 nM ^{32}P-labeled RNA, 25 mM HEPES (pH 7.4), 150 mM potassium acetate, 5 mM magnesium acetate, and 6% glycerol. A series of protein concentrations were tested in binding affinity studies. RNA was prewarmed to 90°C for 2 min and then allowed to cool to room temperature for 3 min before addition to the protein-buffer mixture. After the addition of RNA, the mixtures were subjected to a vortex for 2 s and then centrifuged briefly to remove aggregates. Samples were incubated for 5 min and then loaded onto a 6% polyacrylamide gel containing 1× Tris-borate-EDTA buffer. The gel was prerun for 50 min at 500 V in a 1× Tris-borate-EDTA running buffer. Electrophoresis was then carried out at 500 V for 55 min with the temperature regulated by a water bath to maintain 25°C. Gels were dried and exposed to a phosphor storage screen for imaging and quantitation with a Typhoon phosphorimager and ImageQuant software.

RESULTS

The amino acid residues 81 to 113 of the SINV CP have been implicated in the initial steps of NC assembly, as well as in disassembly following virus infection of new cells (9, 29, 35, 39). Amino acids 97 to 106 influence the recognition of an

encapsidation signal on the genomic RNA, while amino acids 107 to 113 have been implicated in the assembly process at a step other than RNA genome binding (22, 33, 35) (16, 26, 28). Previously, point mutations in the region of amino acids 97 to 106 yielded viruses without apparent growth defects. However, a deletion of residues 97 to 106 results in a virus that has lost its encapsidation specificity (22). Therefore, a comprehensive deletion analysis of the region was carried out to identify residues that are involved in NC assembly, the specific encapsidation of the genomic RNA, or both.

Viruses lacking amino acids 96 to 113 have replication defects. Mutant viruses were generated by the transfection of BHK cells with infectious RNA. These viruses were characterized initially by their plaque sizes at 48 h postinfection to determine if they had any obvious defects in replication (Fig. 1A). These analyses showed that the deletion of 5 or 10 amino acids within the region from positions 81 to 95 resulted in viruses with wild-type plaque sizes. The deletion of the conserved region from positions 96 to 100 resulted in a virus that had medium-sized plaques, while the remaining deletions all resulted in viruses with small plaques, suggesting defects in virus growth. To quantify these observations and to determine if any of the large-plaque viruses had subtle defects, one-step growth analyses of all the mutants were conducted. These analyses showed that the large-plaque viruses CΔ(81–85), CΔ(86–90), CΔ(81–90), and CΔ(91–95) displayed growth characteristics similar to those of the wild type (data not shown). The medium-plaque virus CΔ(96–100) had reduced growth compared to the growth of the wild-type virus starting at 3 h postinfection (Fig. 2). Interestingly, the larger-deletion mutant CΔ(91–100) had more significantly reduced replication than one would expect based on the phenotypes of the CΔ(91–95) and CΔ(96–100) mutants, suggesting some level of synergy between residues 91 to 95 and 96 to 100. The level of small-plaque-virus growth ranged from 1 to 10% of that of the wild-type virus at each time point. These observations suggest that deletions within the region from positions 91 to 113 cause defects in virus replication, resulting in a reduction in the number of infectious virions being produced, while amino acid residues 81 to 95 are dispensable for the virus life cycle. As the region from 91 to 113 has previously been implicated in both genomic RNA encapsidation and NC assembly, it was necessary to determine if the growth defects observed in the mutants were due to deficiencies in either one or both of these functions.

Amino acids 106 to 113 are responsible for NC accumulation. CP mutations were characterized for their role in NC assembly by the measurement of the relative amounts of NCs that accumulated in the cytoplasm of infected cells. Briefly, BHK cells were electroporated with RNA so that potential entry or disassembly defects did not affect the results. The electroporation efficiency was determined to be greater than 90% by immunofluorescence assays probing for the presence of glycoprotein E2. Newly produced viral RNA was labeled with [5,6-^{3}H]uridine. Cytoplasmic extracts were harvested at 12 h postelectroporation and subjected to sedimentation in 10 to 40% sucrose density gradients, followed by fractionation. The amount of radioactivity in each fraction was measured to determine the amount of viral RNA present, while Western blotting was performed to determine the amount of CP. NCs

sedimented as a peak in fractions 2 to 6 (22). The area under the peak represented the amount of labeled viral RNA in NCs. The mutations tested corresponded to a range of phenotypes, with labeled-RNA levels from approximately 80% of the wild-type level in the case of CΔ(96–100) to undetectable levels (Table 1). In every case in which NCs were observed, CP levels in the peak fraction were similar to wild-type levels, suggesting that the amount of NCs accumulated was close to the level for the wild type (data for a subset of mutants are shown in Fig. 3). In every case in which accumulated NCs were not observed, no or very little CP was detected in the fractions, showing that NC accumulation was below detectable levels.

Amino acids 96 to 113 are responsible for the specific encapsidation of genomic RNA. CΔ(96–100) and CΔ(101–105) have wild-type levels of NC assembly, as shown by Western blots (Fig. 3 and data not shown), but lower-than-wild-type levels of viral RNA encapsidated within the NCs (Table 1). In vitro assembly experiments using a variety of nucleic acid lengths demonstrated previously that the NC assembles with approximately a genome equivalent of RNA, and it was suggested that this finding was a result of charge neutralization of the CPs (32). Thus, if one proposes that these NCs contain genome equivalents of RNA, there is a substantial fraction of mutant CPs that presumably package nonviral, or host, RNAs. Therefore, it can be concluded that these mutants have encapsidation defects. This has been shown previously in the case of CΔ(97–106) (22). Due to the difficulty of probing for random nonviral RNAs in the released mutant virus particles, the loss of RNA encapsidation specificity was determined by assaying for the presence of viral genomic and subgenomic RNAs in these particles. In a wild-type infection, less than 5% of encapsidated RNA is subgenomic RNA, while in the CΔ(97–106) infection, the subgenomic RNA is encapsidated at a rate of five subgenomic RNA molecules to one genomic RNA molecule (22).

A qRT-PCR method was developed to determine the amounts of genomic and subgenomic RNAs in each virus sample. Briefly, supernatants containing virus released from infected cells were subjected to two qRT-PCR assays, one to measure the amount of genomic RNA and another to measure the amount of subgenomic RNA. Each assay was conducted in triplicate, the results were averaged, and the ratio of subgenomic RNA to genomic RNA was determined. The means of the results are depicted in Fig. 4. The C_T values determined by qRT-PCR were converted into numbers of molecules of RNA by using a standard curve based on known amounts of in vitro-transcribed and purified viral genomic RNA. There is a slight overestimation of the amount of subgenomic RNA in the assays due to the errors in the qRT-PCR assay results' being magnified by the conversion of C_T values into numbers of molecules of RNA. For example, a difference of 0.2 in C_T between the genomic and subgenomic values, which is typically observed, leads to the subgenomic RNA/genomic RNA ratio's being 0.4 for the wild type. Any mutation that causes a loss of encapsidation specificity is predicted to yield the encapsidation of subgenomic and genomic RNAs at a ratio similar to that at which these RNAs are present in the cytoplasm of infected cells. However, there are other factors that may impact this prediction. In order to neutralize the basic charge on 240 copies of CP, each assembled NC is expected to have a core-

A

Region I   Region II   Region III

```
          1        38  56   81       114                          264
        N  +++++ |   | +++ |      |                              | C
              Helix I
                              81    86      91    96    101   106   111
          WT    K P K K P K T Q E K K K K Q P A K P K P G K R Q R M A L K L E A D   LP
                40 30 50 40 20 60 10 50 10 90 40 60 40 30 20 50 90 40 90 . . 60 . 50 . 90 20 20 . 30 . 20 .

CΔ(81-85)    Δ Δ Δ Δ Δ . . . . . . . . . . . . . . . . . . . . . . . . . . . .   LP
CΔ(86-90)    . . . . . Δ Δ Δ Δ Δ . . . . . . . . . . . . . . . . . . . . . . .   LP
CΔ(81-90)    Δ Δ Δ Δ Δ Δ Δ Δ Δ Δ . . . . . . . . . . . . . . . . . . . . . . .   LP
CΔ(91-95)    . . . . . . . . . . Δ Δ Δ Δ Δ . . . . . . . . . . . . . . . . . .   LP
CΔ(96-100)   . . . . . . . . . . . . . . . Δ Δ Δ Δ Δ . . . . . . . . . . . . .   MP
CΔ(91-100)   . . . . . . . . . . Δ Δ Δ Δ Δ Δ Δ Δ Δ Δ . . . . . . . . . . . . .   SP
CΔ(101-105)  . . . . . . . . . . . . . . . . . . . . Δ Δ Δ Δ Δ . . . . . . . .   SP
CΔ(106-110)  . . . . . . . . . . . . . . . . . . . . . . . . . Δ Δ Δ Δ Δ . . .   SP
CΔ(101-110)  . . . . . . . . . . . . . . . . . . . . Δ Δ Δ Δ Δ Δ Δ Δ Δ Δ . . .   SP
CΔ(97-106)   . . . . . . . . . . . . . . . . Δ Δ Δ Δ Δ Δ Δ Δ Δ Δ . . . . . . .   SP
CΔ(107-113)  . . . . . . . . . . . . . . . . . . . . . . . . . . Δ Δ Δ Δ Δ Δ Δ   SP
K99E         . . . . . . . . . . . . . . . . . . E . . . . . . . . . . . . . .   MP
R103A        . . . . . . . . . . . . . . . . . . . . . . A . . . . . . . . . .   MP
R105A        . . . . . . . . . . . . . . . . . . . . . . . . A . . . . . . . .   MP
R105E        . . . . . . . . . . . . . . . . . . . . . . . . E . . . . . . . .   MP
R103A/R105A  . . . . . . . . . . . . . . . . . . . . . . A . A . . . . . . . .   MP
K99E/R105E   . . . . . . . . . . . . . . . . . . E . . . . . E . . . . . . . .   MP
L108D        . . . . . . . . . . . . . . . . . . . . . . . . . . . D . . . . .   MP
L110N        . . . . . . . . . . . . . . . . . . . . . . . . . . . . . N . . .   MP
L108D/L110N  . . . . . . . . . . . . . . . . . . . . . . . . . . . D . N . . .   MP
```

B

```
                                    A       A                   A
                                    A       A           A       A
         K P K K P K T Q E K K K K Q P A K P K P G K R Q R M A L K L E A D
           A       A   A           A   A   A A   A A A A       A A A
                                           L               L
                                           M               M
                                           R               K
                                           E               E
```

FIG. 1. Mutations in the SINV CP. (A) Schematic of the CP. Amino acids 1 to 37 and 56 to 80 are involved in charge neutralization of the genomic RNA. Amino acids 38 to 55 comprise helix I. Amino acids 81 to 113 comprise the specific RNA binding region. Amino acids 114 to 264 fold into a serine autoprotease. Amino acids in the region from positions 81 to 113 are represented in this figure. The numbers above the residues indicate the amino acid numbers, while the numbers below the sequence indicate the percentage of identity at each position in sequences from alphaviruses Aura, Chikungunya, Eastern equine encephalitis, Mayaro, O'Nyong Nyong, Ross River, Semliki Forest, Venezuelan equine encephalitis, and Western equine encephalitis viruses. Periods indicate no change from the original amino acid. Plaque sizes were determined by estimating the mean diameter of 20 plaques counted per virus. LP, large plaque (5-mm diameter); MP, medium plaque (3-mm diameter); SP, small plaque (2-mm diameter). (B) Single and double substitutions in peptide CP(81–112). Shown below the sequence are single substitutions for each residue. Underlined residues above the sequence indicate sites of double substitutions.

filled complement of RNA (32). This arrangement can occur only by the encapsidation of three molecules of subgenomic RNA. Therefore, the encapsidation of one molecule of subgenomic RNA will make it likely that two more molecules of RNA are encapsidated. This situation can change the expected ratio of subgenomic and genomic RNAs to greater than 9 in the case of a complete loss of specificity. Due to the aforementioned error in C_T determination, the values determined for
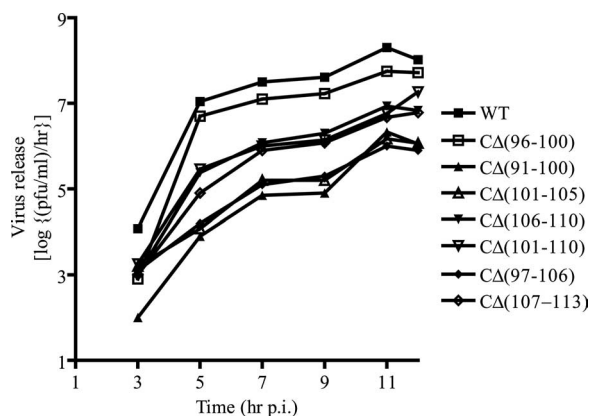
FIG. 2. One-step growth analyses of deletion mutants. BHK cells were infected at a multiplicity of infection of 2 with either wild-type (WT) or mutant viruses. The cells were then washed with Eagle's minimal essential medium supplemented with 5% fetal bovine serum once every 30 min over 2 h for a total of four washes. Supernatant was collected every hour, and the medium was replaced with fresh medium. Supernatants from 3, 5, 7, 9, 11, and 12 h postinfection (p.i.) were assayed by plaque titration. Growth curve analyses were performed twice, and the mean titer values are shown.

FIG. 3. Selected data from NC accumulation assays. Fraction numbers denote fractions from the bottom to the top of a 10 to 40% sucrose density gradient. The graph shows [3H]uridine counts per minute, while the gels depict the amount of CP in each fraction as measured by Western blotting. WT, wild type.

subgenomic and genomic RNAs are not absolute and are relative to the values seen for the wild type. CΔ(97–106) showed the highest amount of subgenomic RNA packaged in relation to the amount of genomic RNA, encapsidating 11 times as much subgenomic RNA. The mutant virus CΔ(101–105) encapsidated twice the amount of subgenomic RNA as genomic RNA. This virus behaved identically to CΔ(97–106) in growth experiments as well as in the NC accumulation assay, leading to the suggestion that the defect observed in CΔ(97–106) was due primarily to the deletion of amino acids 101 to 105.

CΔ(106–110) had a subgenomic/genomic RNA ratio of 3.4. This ratio was similar to the subgenomic/genomic RNA ratio in infected cells. The other deletion mutants not discussed previously, CΔ(96–100), CΔ(91–100), CΔ(101–110), and CΔ(107–113), had values ranging between 1.1 and 2.2. These results

TABLE 1. NC accumulation

Virus	Level of [3H]RNA in NC (% of wild-type level)[b]
Wild type[a]	100
CΔ(96–100)	78 ± 3
CΔ(91–100)	<5
CΔ(97–106)	35 ± 2
CΔ(101–105)[a]	36 ± 3
CΔ(101–110)	<5
CΔ(106–110)	<5
CΔ(107–113)[a]	<5
K99E	71 ± 4
R103A	100 ± 2
R105A	100 ± 4
K99E/R105E	63 ± 7
R103A/R105A	<5
L108D	<5
L110N	<5
L108D/L110N	<5

[a] Data are shown in Fig. 3.
[b] Values are means ± standard deviations.

may be explained by a reduction in specific encapsidation in these mutants, although they still retained some specificity for genomic RNA.

Amino acids 99 and 105 of CP may interact directly with the encapsidation signal. Interpretations of the effects of deletions on protein function are inherently difficult. The deletion of amino acids results in both the removal of the selected residues and a change in the structure of the region. Therefore, it is unclear if the phenotypes observed are due to the removal of functional residues or to a change in the orientation or position of the amino acids that determine the specificity of encapsidation and NC accumulation. In addition, since the encapsidation data are determined from released viruses, they do not measure the direct binding of CP to the encapsidation signal on the genomic RNA. To determine the role of amino acids from CP region II in encapsidation, a previously developed mobility shift assay (14) was used to characterize the binding of a small RNA fragment containing the encapsidation signal to a CP fragment possessing amino acid residues 81 to 112 of the SINV CP. This assay was used in conjunction with alanine scanning mutagenesis to identify amino acid residues important for the recognition and packaging of the viral genome. The residues examined by alanine substitution are shown in Fig. 1B. Each of the mutant peptides was purified and then analyzed by the native gel mobility shift assay to determine which substitutions altered the ability of that mutant peptide to bind encapsidation signal RNA. For each substitution, binding at different concentrations of CP was quantified and the results were plotted, allowing the approximation of the apparent dissociation constants by fitting the data to the Hill equation (Table 2). Of the substitutions examined, only alanine substitutions for K99 and R105 resulted in decreased affinity. The lack of binding saturation for these mutants prevented their saturation curves from being fit to a binding model. Thus, the affinities recorded in Table 2 for these two substitutions were estimated by measur-
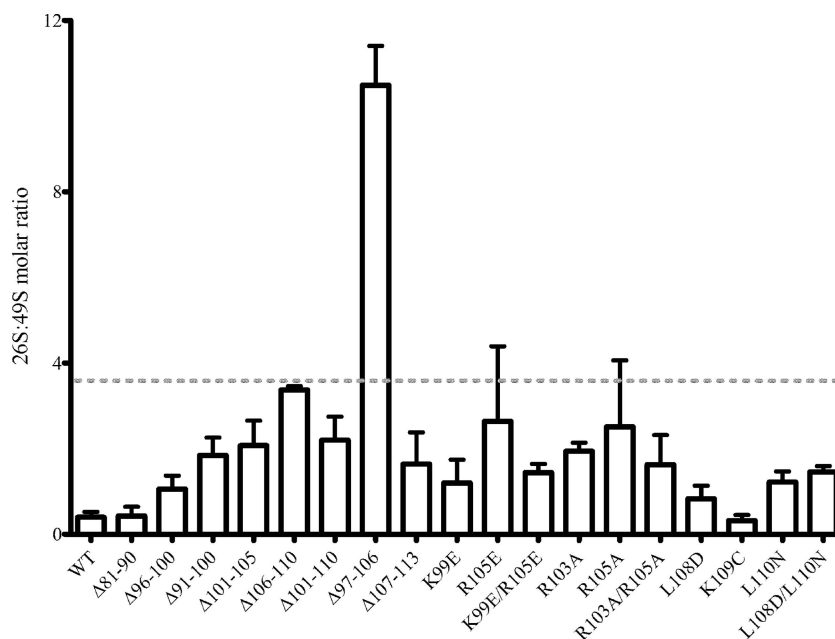
FIG. 4. Ratio of subgenomic RNA to genomic RNA in viruses containing mutant CPs. qRT-PCR assays were conducted with supernatants from cells infected with wild-type (WT) or mutant viruses. The assays determined the numbers of molecules of subgenomic and genomic RNAs in each sample. Ratios of subgenomic RNA to genomic RNA were determined by dividing the number of subgenomic RNA molecules by the number of genomic RNA molecules in each sample. Each experiment was performed three times, with three repetitions for each sample. The horizontal dashed line shows the ratio of subgenomic RNA to genomic RNA present in the cytoplasm of infected cells at 10 h postinfection relative to the ratio in wild type-infected cells.

TABLE 2. Binding affinities of CP(81–112) alanine mutant peptides for encapsidation signal RNA

CP peptide	Avg K_d^{app} (nM)[a]
Wild type	12 ± 2
K83A	12 ± 1
K86A	9 ± 1
Q88A	14 ± 2
K92A	19 ± 2
Q94A	13 ± 3
K97A	13 ± 2
K99A	>100
K99L	>100
K99M	10 ± 2
K99R	8 ± 2
K99E	>100
P100A	14 ± 2
K102A	8 ± 2
R103A	8 ± 2
Q104A	13 ± 3
R105A	>100
R105L	>100
R105M	>100
R105K	9 ± 2
R105E	>100
L108A	4 ± 2
K109A	10 ± 1
L110A	10 ± 1
K97A/K99A	>100
K99A/R105A	>100
R103A/R105A	>1000

[a] K_d^{app}, apparent dissociation constant. Values are means ± standard deviations.

ing the peptide concentration at which half of the free RNA was moved into a complex. This method provides only an estimation of the affinity since the observed binding fails to saturate at higher concentrations of protein, as demonstrated in Fig. 5. This situation is analogous to the nonspecific binding observed for the interaction of the native peptide sequence with RNAs with unrelated sequences (14). It suggests that these mutant peptides have lost the ability to specifically bind the encapsidation signal RNA.

To better understand the functional role of amino acid residues K99 and R105, they were subjected to further mutational analysis. The series of substitutions used was developed to determine if the decrease in binding affinity of the CP for RNA was due to the loss of an important functional group from the side chain of these residues. Alternatively, the loss of binding affinity could be due to improper folding. For this analysis, each residue was individually mutated to leucine, methionine, glutamate, and either lysine or arginine depending on the identity of the original residue. Leucine or methionine substitutions were performed to determine if binding was restored by the placement of a side chain smaller than the original side chain at the analyzed position. The restoration of binding by these substitutions would suggest that the side chain plays a solely structural role in the molecule and that the replacement with alanine had produced a structural deficiency that interfered with the proper folding of the peptide. Replacements with glutamate and either lysine or arginine focused on whether the charge of the side chain is important for binding. The dissociation constants for the binding of each of these mutant peptides as determined in vitro using the CP(81–112) peptide are reported in Table 2.
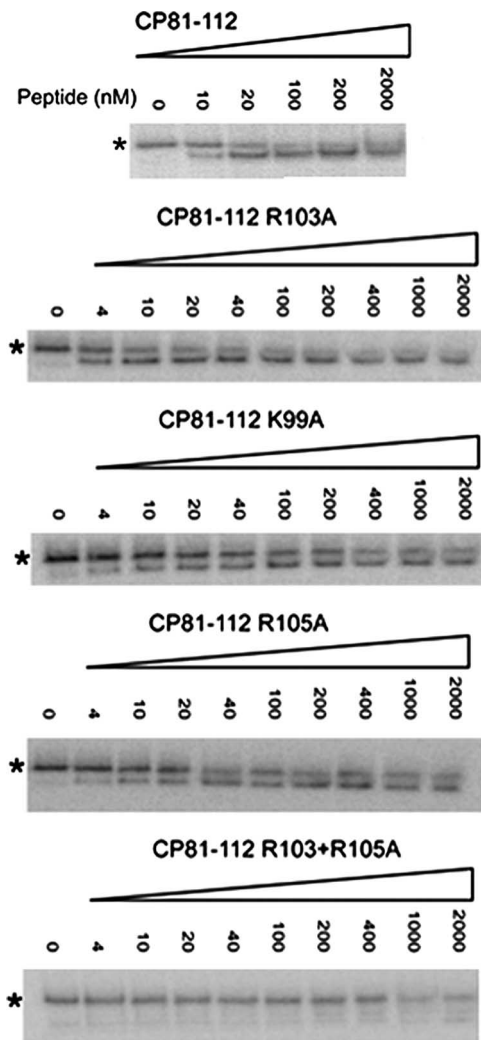
FIG. 5. Results from mobility shift assays of the binding of CP(81–112) alanine mutant peptides to encapsidation signal RNA. Native gel mobility shift assays compared the encapsidation signal RNA binding levels observed for four different CP(81–112) alanine mutant proteins: the K99A, R103A, R105A, and R103A/R105A proteins. Increasing amounts of protein were mixed with 0.2 nM RNA labeled with [^{32}P]CTP at the 5′ end, as indicated. Samples were loaded onto a nondenaturing 6% polyacrylamide gel to allow the separation of protein-bound complexes from unbound RNA. The asterisks indicate the mobility of free RNA.

At position 99, mutation to leucine or glutamate resulted in at least a 10-fold decrease in the affinity of binding whereas replacements with methionine or arginine were tolerated. At residue 105, mutation to leucine, methionine, or glutamate disrupted binding, reducing the affinity by at least 10-fold, while replacement with lysine was tolerated, demonstrating no effect on specific RNA binding affinity. Together, these results suggest that the positive charge of the residues at positions 99 and 105 is of primary importance to specific RNA binding.

In addition to the single-site substitutions, two double mutants in which alanine was substituted at two positions simultaneously (mutants K97A/K99A and R103A/R105A) were tested for their affinities for the encapsidation signal RNA. These mutants were designed to examine the effect of remov-

ing multiple highly conserved positively charged residues and were targeted at the two sites observed to be important in the single-substitution analyses. Each of these mutants demonstrated reduced binding affinity in the in vitro binding assay. The double mutant K97A/K99A exhibited a 10-fold-reduced binding affinity compared to that of the wild type. The R103A/R105A mutant, however, demonstrated a 100-fold decrease in the binding. This result was surprising because it failed to correlate with the combined effect of each of the single-site mutations R103A and R105A. The affinity observed for mutant K97A/K99A correlated with the affinity that would be expected from combining each of the two single-site substitutions K97A and K99A. Since mutant K99A possessed weaker affinity than the wild type for binding encapsidation signal RNA and mutant K97A did not, the weaker binding observed for the double mutant was due solely to the substitution at position 99.

The in vitro binding analyses showed that residues K99, R103, and R105 were critical for specific encapsidation. Thus, these three may be the primary amino acids that are involved in determining encapsidation specificity. In this case, based on the phenotypes observed with deletion mutants CΔ(96–100), CΔ(101–105), and CΔ(97–106), mutations at positions 99, 103, and 105 of CP are predicted to cause encapsidation defects but no defects in NC assembly. Table 1 shows the results of the core accumulation assays conducted with mutants K99E, K99E/R105E, R103A, R105A, and R103A/R105A. K99 and R105 were mutated to aspartic acid so as to reverse the charge of the side chain and create repulsion between the side chain and the interacting RNA. K99E and K99E/R105E mutants accumulate wild-type levels of NCs while still encapsidating approximately 65% viral RNA. The encapsidation phenotype predicted by NC accumulation data was confirmed by the determination of the subgenomic/genomic RNA ratios, which were 1 for mutant K99E, 2 for mutant R105E, 2 for mutant R105A, and 1 for mutant K99E/R105E. In the qRT-PCR assay, the standard deviations among three replicates of the samples of mutants R105A and R105E were high compared to those of the other mutants; however, it is expected that mutants that lose specificity in encapsidation package different amounts of subgenomic RNA in different preparations. This characteristic leads to the high standard deviation when the results from independently amplified virus samples are averaged. These assembly and encapsidation results are consistent with the hypothesis that K99 and R105 are directly involved in the encapsidation of the genomic RNA. Therefore, the encapsidation deficiency of CΔ(96–100) is likely to be due to the loss of K99. It should be pointed out that a previous analysis of the R105A mutant failed to detect a defect in genome recognition (22). However, that study looked simply at the plaque phenotype and did not detect significant plaque size differences from the wild type, in contrast with the results presented here.

Previous studies had shown that L108D and L110N as single or double mutations disrupt NC accumulation (13). In order to determine if the residues at positions 108 and 110 have a role in specific encapsidation, the subgenomic/genomic RNA ratio within released virus particles was determined (Fig. 4). In each case, there was a modest loss of specific encapsidation, with the mutants encapsidating more subgenomic RNA than the wild type but less subgenomic RNA than CΔ(97–106). Since the CP(81–112) peptide with the L108A mutation [CP(81–112)

TABLE 3. Summary of capsid mutant phenotypes

Virus	Core accumulation	Encapsidation specificity[a]
Wild type	Yes	Yes
CΔ(96–100)	Yes	No
CΔ(91–100)	No	No
CΔ(101–105)	Yes	No
CΔ(106–110)	No	No
CΔ(101–110)	No	No
CΔ(97–106)	Yes	No
CΔ(107–113)	No	No
K99E	Yes	No
K99E/R105E	Yes	No
R103A	Yes	No*
R105A	Yes	No
R103A/R105A	No	No
L108D	No	No*
L110N	No	No*
L108D/L110N	No	No*

[a] Asterisks indicate that, in these mutants, the binding affinities of the CP(81–112) mutant proteins for the encapsidation signal RNA were not significantly affected relative to the affinity of the wild-type protein.

L108A] and CP(81–112) L110A displayed wild-type affinities of binding to the encapsidation signal sequence RNA, it is unlikely that L108 and L110 interact directly with the RNA. Therefore, the observed encapsidation defect was likely due to factors that do not include direct interactions with the encapsidation signal.

DISCUSSION

Region II of the SINV CP (amino acids 81 to 113) has been implicated previously in the specific encapsidation of the genomic RNA and in CP-CP dimer formation following nucleic acid interaction (9, 14, 16, 22, 28, 29, 35, 36). The present studies were conducted to evaluate whether the regions of amino acids that determine each function are discrete or overlapping. Deletion mutations throughout region II were made, and the resulting viruses were characterized for defects in NC assembly or specific encapsidation of genomic RNA. The role of specific amino acids within this region in encapsidation was unclear. To determine whether any of the residues within region II interacted with the encapsidation signal on the genomic RNA directly, mobility shift assays were carried out with peptide CP(81–112) and the encapsidation signal of the genomic RNA. The binding abilities of mutant peptides with alterations at various positions of CP(81–112) were characterized, and the mutations corresponding to those peptides that were defective in binding to the encapsidation signal sequence RNA were introduced into the full-length cDNA for further characterization of growth, NC accumulation, and the presence of subgenomic RNA in the resulting viruses. Table 3 provides a summary of the capsid mutant phenotypes.

Deletions in the region from positions 81 to 95 of the SINV CP produced viruses with growth characteristics identical to those of the wild type. In support of this observation, single amino acid replacements of residues K83, K86, E88, K92, and Q94 with alanine in the CP(81–112) peptide resulted in no significant decrease in binding affinity for the encapsidation signal. Therefore, it can be concluded that either the amino

acid region from 81 to 95 does not play any significant role in virus assembly or it can be functionally replaced by surrounding amino acids. If the former is true, then this region is likely to be involved in charge neutralization of the viral RNA and its loss will not cause significant defects. If the latter is true, then the surrounding region is flexible and can undergo the dynamic interactions that lead to the assembled NC. In contrast, deletions and substitutions in the region from 96 to 113 caused defects in the replication of the virus, with the residues at positions 96 to 106 implicated in packaging specificity and the residues at positions 97 to 113 implicated in core assembly.

Various studies, including this one, have shown that the ratio of subgenomic RNA to genomic RNA inside cells infected with SINV at 10 h postinfection is approximately 3:1. The wild-type CP shows specificity by incorporating more than 95% genomic RNA into the virions. Any mutant CP that causes a loss of specificity in RNA recognition would be expected to incorporate subgenomic and genomic RNAs at the same ratio at which these RNAs are present at the site of NC assembly. However, it is also possible that the encapsidation of one molecule of subgenomic RNA results in the encapsidation of two more molecules of subgenomic RNA in order to keep the amount of charge inside the NC similar to that of the wild type. Therefore, a mutant having a complete loss of specificity in genomic RNA encapsidation may be expected to encapsidate at least nine times more subgenomic RNA than genomic RNA. The previously described mutant CΔ(97–106) incorporates 11 times more subgenomic RNA than genomic RNA into virions, while the other mutants encapsidated RNAs at a ratio of less than 3. In particular, CΔ(101–105) showed growth and NC accumulation phenotypes similar to those of CΔ(97–106). However, the ratios of subgenomic RNA to genomic RNA in these two mutated viruses were not similar. CΔ(101–105) encapsidated twice as much subgenomic RNA as genomic RNA. This finding suggests that the encapsidation phenotype observed in CΔ(97–106) was not due simply to a loss of specificity for genomic RNA. The most likely possible explanation for the higher levels of encapsidation of subgenomic RNA by CΔ(97–106) than by CΔ(101–105) is that the deletion in CΔ(97–106) leads to a preference for the encapsidation of RNAs that are smaller than the genomic RNA. The analysis of a naturally occurring second-site revertant of CΔ(97–106) that has a duplicate of the amino acid region from positions 10 to 89 lends support to this idea. The revertant has partially restored ability to encapsidate the genomic RNA, without altered specificity for the encapsidation signal on the genomic RNA. Additional charge neutralization is available in the case of the CP in this virus, and so the CP encapsidates the larger RNA (21). Another possibility is that, in wild-type virus, there is a mechanism for the CP to be transported to the site of genomic RNA replication from the site of CP synthesis and that this process is disrupted in CΔ(97–106). This disruption would cause the CP to remain associated with subgenomic RNA after translation and preferentially encapsidate the subgenomic RNA into NCs. If this mechanism has been disrupted in CΔ(97–106) but not in CΔ(101–105), then the observed phenotypes can be explained. The post-translational interaction of CP with the ribosome may serve to transport CP to areas of genomic RNA production. For those mutants that did not accumulate NCs in the cytoplasm, i.e., CΔ(91–100), CΔ(101–110), and CΔ(107–113),

the NC assembly phenotype may have influenced the encapsidation specificity.

The initial round of alanine scanning mutagenesis identified two amino acid residues, K99 and R105, that are important for binding the encapsidation signal of the viral RNA. Further mutational analysis of positions 99 and 105 revealed that maintaining basic amino acids at each position was important for specific RNA binding. Interestingly, these two positions both reside within the CP region from positions 97 to 106. Among 10 alphaviruses, 90% of the residues at position 99 are identical and 100% of the residues at positions 103 and 105 are identical. Many other amino acids among residues 97 to 113 are conserved among members of the *Alphavirus* genus. Single mutants R103A and R105A showed no defects in NC accumulation; however, surprisingly, the double mutant R103A/R105A did not accumulate any NCs. All three mutants had encapsidation defects, which were unexpected based on the single-mutant results. The NC accumulation assay discriminates only between labeled viral and unlabeled nonviral RNAs and not between the subgenomic and genomic RNAs. The results suggest that R103A and R105A mutants do not encapsidate host cell RNAs but that they do have an encapsidation defect resulting in subgenomic RNA's being packaged into the virions. The NC accumulation phenotype of mutant R103A/R105A suggests that R103 and R105 have redundant functions in assembly such that if only one of the two arginines is missing, NC accumulation occurs, but if both are missing, the functional role of the arginines is not replaced by any other amino acid. The double mutant has a more severe defect than the deletion mutant CΔ(101–105), which lacks amino acids R103 and R105 and yet accumulates NCs.

When the crystal structure of the SINV CP was fitted into the cryoelectron microscopy density map of the mature virus particle, amino acid residues 97 to 113 were modeled as an α-helix into a strand of density spanning the distance between the outer capsomeres and the inner RNA-protein layer of the NC (4, 19). Assuming that the residues 106 to 113 are in a native configuration in the crystal structure, this orientation indicates that in the mature NC, residues 97 to 113 are no longer in contact with either the RNA genome or CP. The results of the present study strongly indicate that there is interaction between residues 97 to 113 and RNA during the initial stages of NC assembly. If the direct interaction of K99, R103, and R105 with the encapsidation signal sequence is important to the formation of the initiation complex for the specific packaging of the viral RNA genome, as suggested by the interaction of peptide CP(81–112) with RNA, then a structural change occurs prior to the completion of NC assembly, as this interaction does not exist in the released virus. This finding suggests that the CP dimer that forms to provide specific recognition of the RNA genome and nucleate the assembly process is no longer present in the assembled NC. Given that the interactions between amino acids K99, R103, and R105 and the encapsidation signal of the RNA are high-affinity ones, this reorganization may prime the NC for disassembly following viral entry into a new cell. Coombs et al. previously showed such a conformational change to occur in the alphavirus NC (5, 6).

Taken together, these data suggest that factors other than direct interaction with the genomic RNA play a role in the encapsidation of the RNA. One of these factors may be that there are multiple binding sites for CP on the genomic RNA and the conserved residues that do not interact with the encapsidation signal interact with these other sites during the encapsidation process. An example of this scenario is found in Aura virus, which was determined previously to encapsidate subgenomic RNA in large amounts (26, 27). Several elegant studies have established that SINV CP specifically encapsidates genome RNA containing a packaging signal (8, 13, 35, 36). However, in vitro assembly experiments as well as in vivo analyses of phenotypic mixing suggest that this specificity is not absolute (2, 11, 31, 37, 40). The intracellular environment in which translation, RNA replication, and capsid assembly occurs presumably plays a guiding role in the delivery of appropriate RNA to the site of NC assembly. Subtle differences in RNA binding to the CP may explain specificity and may also explain why other RNA sequences can be packaged, especially in the absence of the genome-packaging signal. The ease with which amino acids suggested to be involved in packaging specificity can be removed or altered without a complete loss of infectivity suggests that this feature is not absolutely required by the virus but that its presence enhances the infectivity of virions.

A detailed model for NC assembly is not yet available but presumably would require residues 99, 103, and 105 of a single CP binding to the encapsidation signal on the genomic RNA as the initial assembly event. This initial nucleation event would promote the formation of a CP dimer, which presumably also requires the interaction of helix I from each individual CP to stabilize the dimer. The region immediately downstream of residues 99, 103, and 105, which is defined by CΔ(107–113), appears to play a major role in NC assembly independent of any contribution to packaging specificity. The subsequent steps for the oligomerization and formation of the T=4 icosahedral NC remain unknown and are the focus of future investigations.

REFERENCES

1. **Aliperti, G., and M. J. Schlesinger.** 1978. Evidence for an autoprotease activity of Sindbis virus capsid protein. Virology **90:**366–369.
2. **Burge, B. W., and E. R. Pfefferkorn.** 1966. Phenotypic mixing between group A arboviruses. Nature **210:**1397–1399.
3. **Cheng, R. H., R. J. Kuhn, N. H. Olson, M. G. Rossmann, H. K. Choi, T. J. Smith, and T. S. Baker.** 1995. Nucleocapsid and glycoprotein organization in an enveloped virus. Cell **80:**621–630.
4. **Choi, H.-K., S. Lee, Y.-P. Zhang, B. R. McKinney, G. Wengler, M. G. Rossmann, and R. J. Kuhn.** 1996. Structural analysis of Sindbis virus capsid mutants involving assembly and catalysis. J. Mol. Biol. **262:**151–167.
5. **Coombs, K., B. Brown, and D. T. Brown.** 1984. Evidence for a change in capsid morphology during Sindbis virus envelopment. Virus Res. **1:**297–302.
6. **Coombs, K., and D. T. Brown.** 1987. Topological organization of Sindbis virus capsid protein in isolated nucleocapsids. Virus Res. **7:**131–149.
7. **Forsell, K., G. Griffiths, and H. Garoff.** 1996. Preformed cytoplasmic nucleocapsids are not necessary for alphavirus budding. EMBO J. **15:**6495–6505.
8. **Forsell, K., L. Xing, T. Kozlovska, R. H. Cheng, and H. Garoff.** 2000. Membrane proteins organize a symmetrical virus. EMBO J. **19:**5081–5091.
9. **Geigenmüller-Gnirke, U., H. Nitschko, and S. Schlesinger.** 1993. Deletion analysis of the capsid protein of Sindbis virus: identification of the RNA binding region. J. Virol. **67:**1620–1626.

10. **Hong, E. M., R. Perera, and R. J. Kuhn.** 2006. Alphavirus capsid protein helix I controls a checkpoint in nucleocapsid core assembly. J. Virol. **80:** 8848–8855.

11. **Kuhn, R. J., Z. Hong, and J. H. Strauss.** 1990. Mutagenesis of the 3′ nontranslated region of Sindbis virus RNA. J. Virol. **64:**1465–1476.

12. **Kuhn, R. J., H. G. M. Niesters, Z. Hong, and J. H. Strauss.** 1991. Infectious RNA transcripts from Ross River virus cDNA clones and the construction and characterization of defined chimeras with Sindbis virus. Virology **182:** 430–441.

13. **Lee, S., K. E. Owen, H. K. Choi, H. Lee, G. Lu, G. Wengler, D. T. Brown, M. G. Rossmann, and R. J. Kuhn.** 1996. Identification of a protein binding site on the surface of the alphavirus nucleocapsid and its implication in virus assembly. Structure **4:**531–541.

14. **Linger, B. R., L. Kunovska, R. J. Kuhn, and B. L. Golden.** 2004. Sindbis virus nucleocapsid assembly: RNA folding promotes capsid protein dimerization. RNA **10:**128–138.

15. **Lopez, S., J. S. Yao, R. J. Kuhn, E. G. Strauss, and J. H. Strauss.** 1994. Nucleocapsid-glycoprotein interactions required for assembly of alphaviruses. J. Virol. **68:**1316–1323.

16. **Mancini, E. J., M. Clarke, B. E. Gowen, T. Rutten, and S. D. Fuller.** 2000. Cryo-electron microscopy reveals the functional organization of an enveloped virus, Semliki Forest virus. Mol. Cell **5:**255–266.

17. **Milligan, J. F., D. R. Groebe, G. W. Witherell, and O. C. Uhlenbeck.** 1987. Oligoribonucleotide synthesis using T7 RNA polymerase and synthetic DNA templates. Nucleic Acids Res. **15:**8783–8798.

18. **Mossessova, E., and C. D. Lima.** 2000. Ulp1-SUMO crystal structure and genetic analysis reveal conserved interactions and a regulatory element essential for cell growth in yeast. Mol. Cell **5:**865–876.

19. **Mukhopadhyay, S., W. Zhang, S. Gabler, P. R. Chipman, E. G. Strauss, J. H. Strauss, T. S. Baker, R. J. Kuhn, and M. G. Rossmann.** 2006. Mapping the structure and function of the E1 and E2 glycoproteins in alphaviruses. Structure **14:**63–73.

20. **Nicola, A. V., W. Chen, and A. Helenius.** 1999. Co-translational folding of an alphavirus capsid protein in the cytosol of living cells. Nat. Cell Biol. **1:**341–345.

21. **O'Rourke, K., L. E. Perryman, and T. C. McGuire.** 1988. Antiviral, antiglycoprotein and neutralizing antibodies in foals with equine infectious anaemia virus. J. Gen. Virol. **69:**667–674.

22. **Owen, K. E., and R. J. Kuhn.** 1996. Identification of a region in the Sindbis virus nucleocapsid protein that is involved in specificity of RNA encapsidation. J. Virol. **70:**2757–2763.

23. **Paredes, A. M., D. T. Brown, R. Rothnagel, W. Chiu, R. J. Schoepp, R. E. Johnston, and B. V. Prasad.** 1993. Three-dimensional structure of a membrane-containing virus. Proc. Natl. Acad. Sci. USA **90:**9095–9099.

24. **Pastorino, B., M. Bessaud, M. Grandadam, S. Murri, H. J. Tolou, and C. N. Peyrefitte.** 2005. Development of a TaqMan RT-PCR assay without RNA extraction step for the detection and quantification of African Chikungunya viruses. J. Virol. Methods **124:**65–71.

25. **Perera, R., K. E. Owen, T. L. Tellinghuisen, A. E. Gorbalenya, and R. J.**

26. **Kuhn.** 2001. Alphavirus nucleocapsid protein contains a putative coiled coil alpha-helix important for core assembly. J. Virol. **75:**1–10.

26. **Rümenapf, T., D. T. Brown, E. G. Strauss, M. König, R. Rameriz-Mitchel, and J. H. Strauss.** 1995. Aura alphavirus subgenomic RNA is packaged into virions of two sizes. J. Virol. **69:**1741–1746.

27. **Rümenapf, T., E. G. Strauss, and J. H. Strauss.** 1994. Subgenomic mRNA of Aura alphavirus is packaged into virions. J. Virol. **68:**56–62.

28. **Schuffenecker, I., I. Iteman, A. Michault, S. Murri, L. Frangeul, M. C. Vaney, R. Lavenir, N. Pardigon, J. M. Reynes, F. Pettinelli, L. Biscornet, L. Diancourt, S. Michel, S. Duquerroy, G. Guigon, M. P. Frenkiel, A. C. Brehin, N. Cubito, P. Despres, F. Kunst, F. A. Rey, H. Zeller, and S. Brisse.** 2006. Genome microevolution of chikungunya viruses causing the Indian Ocean outbreak. PLoS Med. **3:**e263.

29. **Singh, I., and A. Helenius.** 1992. Role of ribosomes in Semliki Forest virus nucleocapsid uncoating. J. Virol. **66:**7049–7058.

30. **Skoging-Nyberg, U., and P. Liljestrom.** 2001. M-X-I motif of Semliki Forest virus capsid protein affects nucleocapsid assembly. J. Virol. **75:**4625–4632.

31. **Strauss, J. H., and E. G. Strauss.** 1994. The alphaviruses: gene expression, replication, and evolution. Microbiol. Rev. **58:**491–562.

32. **Tellinghuisen, T. L., A. E. Hamburger, B. R. Fisher, R. Ostendorp, and R. J. Kuhn.** 1999. In vitro assembly of alphavirus cores by using nucleocapsid protein expressed in *Escherichia coli*. J. Virol. **73:**5309–5319.

33. **Tellinghuisen, T. L., and R. J. Kuhn.** 2000. Nucleic acid-dependent cross-linking of the nucleocapsid protein of Sindbis virus. J. Virol. **74:**4302–4309.

34. **Tellinghuisen, T. L., R. Perera, and R. J. Kuhn.** 2001. Genetic engineering: principles and methods, vol. 23. Genetic and biochemical studies on the assembly of an enveloped virus, p. 83–112. Plenum Press, New York, NY.

35. **Tellinghuisen, T. L., R. Perera, and R. J. Kuhn.** 2001. In vitro assembly of Sindbis virus core-like particles from cross-linked dimers of truncated and mutant capsid proteins. J. Virol. **75:**2810–2817.

36. **Weiss, B., U. Geigenmüller-Gnirke, and S. Schlesinger.** 1994. Interactions between Sindbis virus RNAs and a 68 amino acid derivative of the viral capsid protein further defines the capsid binding site. Nucleic Acids Res. **22:**780–786.

37. **Weiss, B., H. Nitschko, I. Ghattas, R. Wright, and S. Schlesinger.** 1989. Evidence for specificity in the encapsidation of Sindbis virus RNAs. J. Virol. **63:**5310–5318.

38. **Wengler, G., G. Wengler, U. Boege, and K. Wahn.** 1984. Establishment and analysis of a system which allows assembly and disassembly of alphavirus core-like particles under physiological condition *in vitro*. Virology **132:**401–412.

39. **Wengler, G., D. Würkner, and G. Wengler.** 1992. Identification of a sequence element in the alphavirus core protein which mediates interaction of cores with ribosomes and the disassembly of cores. Virology **191:**880–888.

40. **Zavadova, Z., J. Zavada, and R. Weiss.** 1977. Unilateral phenotypic mixing of envelope antigens between togaviruses and vesicular stomatitis virus or avian RNA tumour virus. J. Gen. Virol. **37:**557–567.

41. **Zhang, W., S. Mukhopadhyay, S. V. Pletnev, T. S. Baker, R. J. Kuhn, and M. G. Rossmann.** 2002. Placement of the structural proteins in Sindbis virus. J. Virol. **76:**11645–11658.